Received: 15 May 2020 | Revised: 2 July 2020 | Accepted: 5 July 2020

DOI: 10.1002/aoc.5942

Applied Organometallic Chemistry WILEY

FULL PAPER

Dinuclear gold(I)-N-heterocyclic carbene complexes: Synthesis, characterization, and catalytic application for hydrohydrazidation of terminal alkynes

Seema Yadav[1] | **Sriparna Ray**[2] | **Ajeet Singh**[3] | **Shaikh M. Mobin**[3] | **Tapta Kanchan Roy**[4] | **Chandrakanta Dash**[1]

[1]Department of Chemistry, School of Chemical Sciences and Pharmacy, Central University of Rajasthan, Bandar Sindri, Ajmer, Rajasthan, 305817, India

[2]Department of Chemistry, School of Basic Sciences, Manipal University Jaipur, Jaipur, Rajasthan, 303007, India

[3]Department of Chemistry, Indian Institute of Technology (IIT) Indore, Simrol, Khandwa Road, Indore, 453552, India

[4]Department of Chemistry and Chemical Sciences, Central University of Jammu, Jammu, 180001, India

Correspondence
Tapta Kanchan Roy, Department of Chemistry and Chemical Sciences, Central University of Jammu, Jammu 180001, India.
Email: tapta.che@cujammu.ac.in

Chandrakanta Dash, Department of Chemistry, School of Chemical Sciences and Pharmacy, Central University of Rajasthan, Bandar Sindri, Ajmer 305817, Rajasthan, India.
Email: ckdash@curaj.ac.in

Funding information
DST-FIST, Grant/Award Number: SR/FST/CSI-257/2014(c); DST-SERB, New Delhi, Grant/Award Number: YSS/2014/000054

Dinuclear gold(I)-N-heterocyclic carbene complexes were developed for the hydrohydrazidation of terminal alkynes. The gold(I)-N-heterocyclic carbene complexes **2a**-**2b** were synthesized in good yields from silver complexes synthesized in situ, which in turn were obtained from the corresponding imidazolium salts with Ag_2O in dichloromethane as a solvent. The new air-stable gold(I)-NHC complexes, **2a**-**2b,** were characterized using NMR spectroscopy, elemental analysis, infrared, and mass spectroscopy studies. The gold(I) complex **2a** was characterized using X-ray crystallography. *Bis*-N-heterocyclic carbene–based gold(I) complexes **2a**-**2b** exhibited excellent catalytic activities for hydrohydrazidation of terminal alkynes yielding acylhydrazone derivatives. The working catalytic system can be used in gram-scale synthesis. In addition, the catalytic reaction mechanism of the hydrohydrazidation of terminal alkynes by gold(I)-NHC complex was studied in detail using density functional theory.

KEYWORDS
DFT study, gold, hydrohydrazidation, mechanism, N-heterocyclic carbene

1 | INTRODUCTION

Gold-catalyzed organic syntheses have attracted much attention as it has wide applications in designing novel building blocks for many biologically active compounds and pharmaceuticals.[1] The synthesis of organic molecules using gold catalysts supported by ancillary ligands such as phosphine and N-heterocyclic carbenes (NHCs) can be performed under mild reaction conditions. The addition of nucleophiles such as amine, hydrazine, hydrazide, and semicarbazide to alkynes is considered as 100% atom economical process for the

synthesis of C–N bonded framework.[2] Various research groups have already described the importance of gold(I)-NHC catalysts for these processes.[1k,m,2d,e,g,3] The catalytic activities of various dinuclear gold complexes have also been investigated, and these complexes have shown excellent catalytic activity compared to mononuclear complexes due to its cooperativity effects.[4] As a part of our study on designing new transition metal–based catalysts for C–C and C-heteroatom bond-forming reactions,[5] we have reported a series of well-defined palladium catalysts supported by *bis*-N-heterocyclic carbene ligands for C–H bond arylation of benzothiazole and domino Sonogahsira coupling/cyclization reaction.[6] Based on an earlier work on catalytic performances of dinuclear complexes, analogs of gold(I) complexes of the *bis*-N-heterocyclic carbene ligands have been synthesized, and their catalytic activity in C-heteroatom bond-forming reactions has been studied.

Keto-*N*-acylhydrazones are used as synthetic intermediates for a variety of medicinal compounds.[7] Due to its significance in therapeutic uses, the development of highly efficient methods remains a crucial challenge in the area. Lewis acid-mediated processes, particularly gold-based catalysis involving the activation of alkynes followed by the addition of nucleophiles, are becoming increasingly popular. Studies on the gold(I)-catalyzed addition of hydrazides to alkynes for the synthesis of acylhydrazone are limited. Recently, Kukushkin and coworkers developed a phosphine-based gold(I) catalyst for hydrohydrazidation of terminal alkynes.[8] The catalyst showed good catalytic activity with 6 mol% catalyst loading under mild conditions. Phosphine ligands were replaced by N-heterocyclic carbenes in many transition metal–catalyzed processes (due to their air and moisture stability and high thermal stability),[9] and thus we became interested in exploring the catalytic activity of our synthesized dinuclear gold(I)-N-heterocyclic carbene (NHC) complexes for hydrohydrazidation of terminal alkynes.

Herein, we report the synthesis, characterization, and catalytic activity of bimetallic gold(I)-NHC complexes **2a** and **2b** (Figure 1). Our dinuclear gold(I)-NHC catalysts efficiently catalyze the synthesis of azylhydrazone derivatives. We carried out the DFT study to understand the catalytic reaction mechanism of the hydrohydrazidation of alkynes by $[(NHC)Au]^+$.

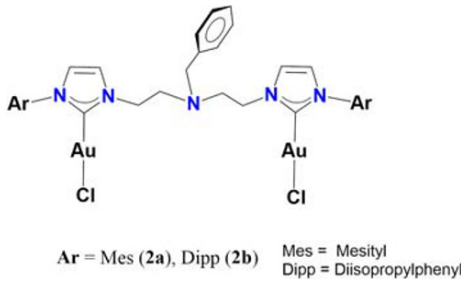

FIGURE 1 Dinuclear gold(I) complexes of N-heterocyclic carbene ligands

2 | RESULTS AND DISCUSSION

2.1 | Synthesis and characterization

NHC-based gold(I) complexes **2a** and **2b** were synthesized in 79% and 85% yields, respectively, from the *in situ*-generated silver complexes (reaction of imidazolium salts with Ag_2O) followed by transmetallation using gold(I) precursor $(SMe_2)AuCl$ (Scheme 1). The gold(I) complexes **2a** and **2b** are stable in air and moisture and could be stored for several months without undergoing any decomposition.

The gold(I) complexes **2a** and **2b** were characterized using various spectroscopic techniques such as ^1H NMR, ^{13}C NMR, high-resolution mass spectrometry (HRMS), infrared spectroscopy, and elemental analysis studies. The $^{13}C\{^1H\}$ NMR spectra of **2a** and **2b** showed a peak at around 171.4 ppm (**2a**) and 172.6 (**2b**), which corresponded to the $Au–C_{carbene}$ peak, similar to the corresponding signal of [1-(benzyl)-3-(2,4,6-trimethylphenyl)imidazol-2-ylidene] AuCl[10] (δ 172.1 ppm). The gold(I) complex **2a** was structurally characterized using X-ray crystallography (Figure 2). The complex **2a** showed linear geometry with two coordinated gold(I) atoms having a bond angle ~180°. The average distances of $Au–C_{carbene}$ and Au–Cl bonds were 1.964 and 2.281 Å, respectively. The distance between two gold(I) atoms was 7.226 Å. Despite all our efforts to grow the crystals in various solvents, we could not obtain suitable crystals of **2b** for X-ray crystallographic study.

2.2 | Hydrohydrazidation of terminal alkynes

Gold(I) catalysts **2a** and **2b** were used for the synthesis of acylhydrazone derivatives, which are essential building

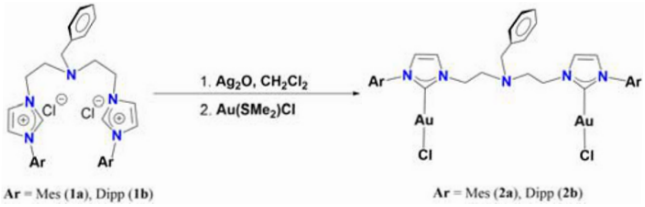

SCHEME 1 Synthesis of dinuclear gold(I)-N-heterocyclic carbene complexes

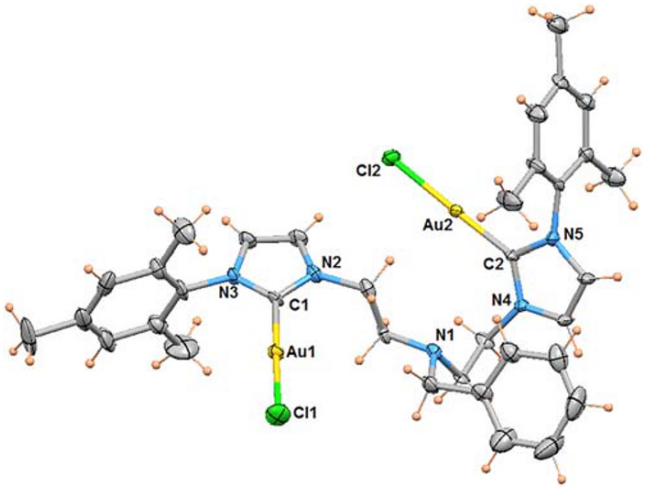

FIGURE 2 Molecular structure of **2a**. Ellipsoids are shown at 30% probability level. Selected bond lengths (Å) and angles (deg): Au1–C1 1.963(9), Au1–Cl1 2.278(3), Au2–C2 1.965(9), Au2–Cl2 2.283(3); C1–Au1–Cl1 178.9(3), N2–C1–N3 103.3(8), C2–Au2–Cl2 178.4(3), N4–Au2–N5 103.7(8)

blocks of many biologically active compounds. Initially, the substrates benzohydrazide and phenylacetylene were used to evaluate the optimum reaction conditions for gold(I)-NHC-catalyzed hydrohydrazidation of terminal alkynes. We first screened with various solvents, temperature conditions, and reaction time using **2a** as a catalyst in addition to the control experiments. Common solvents such as $CHCl_3$, DCE, CH_3CN, EtOH, DMF, 1,4-dioxane, and PhCl were used (Table 1, entries 1–7) for the hydrohydrazidation reaction. The results showed that chlorobenzene is the best solvent and produced the highest product yield, owing to its solubility, the stabilization of the catalytic intermediate, and so on. The effect of phosphine-based catalyst was also studied. Phosphine-based gold(I) precatalyst $(PPh_3)AuCl$ did not show higher catalytic activity compared to gold(I)-NHC complexes **2a** and **2b** either in the same reaction conditions or at low temperature (Table 1, entries 13–14).

The reaction of benzohydrazide with phenylacetylene in chlorobenzene at 95 °C in the presence of 2 mol% of

TABLE 1 Optimization of reaction conditions for hydrohydrazidation of terminal alkynes[a]

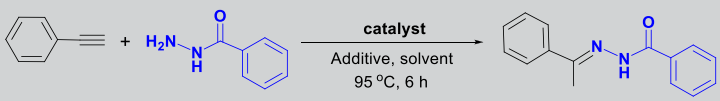

Entry	Catalyst loading (mol%)	Additive (mol%)	Solvent	Yield (%) [b]
1.	**2a** (2.0)	$AgSbF_6$ (4.0)	$CHCl_3$	Trace
2.	**2a** (2.0)	$AgSbF_6$ (4.0)	DCE	26
3.	**2a** (2.0)	$AgSbF_6$ (4.0)	CH_3CN	13
4.	**2a** (2.0)	$AgSbF_6$ (4.0)	EtOH	37
5.	**2a** (2.0)	$AgSbF_6$ (4.0)	DMF	Trace
6.	**2a** (2.0)	$AgSbF_6$ (4.0)	1,4-Dioxane	80
7.	**2a** (2.0)	$AgSbF_6$ (4.0)	PhCl	**>99**
8.	**2a** (1.0)	$AgSbF_6$ (2.0)	PhCl	34
9.	SIPrAuCl (2.0)	$AgSbF_6$ (2.0)	PhCl	40
10.	SIPrAuCl (4.0)	$AgSbF_6$ (4.0)	PhCl	90
11.	IMeAuCl (2.0)	$AgSbF_6$ (2.0)	PhCl	38
12.	IMeAuCl (4.0)	$AgSbF_6$ (4.0)	PhCl	80
13.	Ph_3PAuCl (4.0)	$AgSbF_6$ (4.0)	PhCl	14
14.	Ph_3PAuCl (4.0)	$AgSbF_6$ (4.0)	PhCl	22[c]
15.	**2a** (2.0)	$AgSbF_6$ (4.0)	PhCl	32[c]
16.	**2a** (2.0)	–	PhCl	trace
17.	–	$AgSbF_6$ (4.0)	PhCl	trace

[a]Reaction conditions: benzohydrazide (1.00 mmol), phenylacetylene (1.20 mmol), and solvent (2 mL).
[b]The yields (%) were determined by gas chromatography using 1,3,5-trimethoxybenzene as an internal standard.
[c]Reactions were performed at 60 °C.

TABLE 2 Hydrohydrazidation of terminal alkynes by **2a** and **2b**[a]

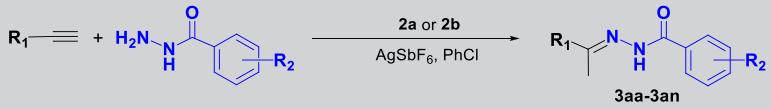

3aa-3an

S.No.	Alkyne	Benzohydrazide	Product	Yield (%)[b] 2a	2b
1.	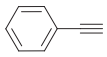	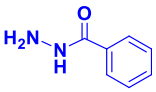	**3aa**	97	96
2.	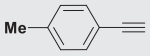	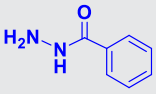	**3ab**	97	99
3.	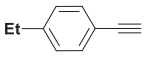	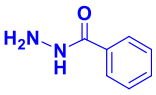	**3 ac**	76	68
4.	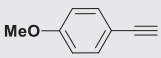	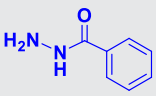	**3ad**	76	87
5.	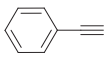	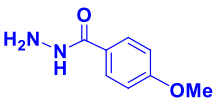	**3ae**	73	69
6.	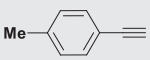	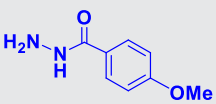	**3af**	67	62
7.	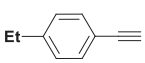	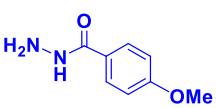	**3ag**	76	66
8.	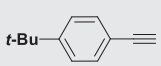		**3ah**	70	71

TABLE 2 (Continued)

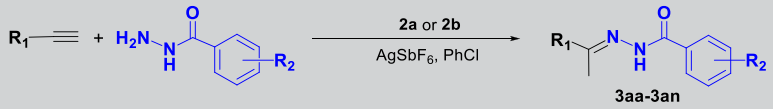

3aa-3an

S.No.	Alkyne	Benzohydrazide	Product	Yield (%)[b] 2a	2b
		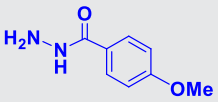			
9.	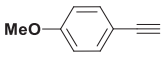	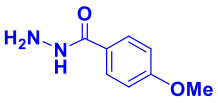	**3ai**	67	59
10.	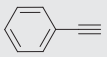	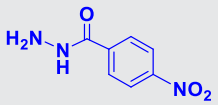	**3aj**	69	64
11.		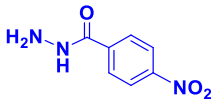	**3ak**	68	63
12.	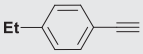	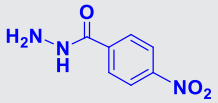	**3al**	61	63
13.	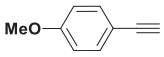	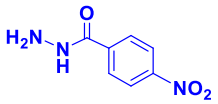	**3am**	66	65
14.		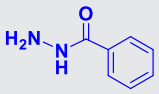	**3an**	37	31

[a]Reaction conditions: benzohydrazide (1.00 mmol), alkyne (1.20 mmol), 2.0 mol% of **2a** or **2b**, $AgSbF_6$ (4.0 mol%), chlorobenzene (2 ml), 95 °C, 6 h.

[b]Yields refer to isolated products.

gold(I)-NHC/4 mol% $AgSbF_6$ resulted in a complete conversion in 6 h in the air (Table 1, entry 7). No acylhydrazone product was observed when the **2a** pre-catalyst was used without the addition of $AgSbF_6$ (Table 1, entry 16).

By using the optimized condition, we explored the various alkyne and benzohydrazide substartes. Benzohydrazide substrates, including the electron-donating (4-$OMeC_6H_4$) and electron-withdrawing group (4-$NO_2C_6H_4$), were tested with several terminal alkynes and resulted in moderate to excellent yields (isolated yield: 59–99%) of acylhydrazone derivatives (Table 2). The functional groups –OMe, $–NO_2$, and –OH were tolerated on both alkynes and hydrazides under the catalytic conditions. The reaction of propargyl alcohol with benzohydrazide synthesized the corresponding product in moderate yield (31–37%), whereas the internal alkyne such as diphenylacetylene showed less product conversion up to 12%. Other aliphatic alkynes such as ethylpropiolate and 1-hexyne yielded hydrazide products in traces. The acylhydrazone product **3aa** was also synthesized in gram-scale in excellent yield, which shows that this catalytic system can be used in large-scale syntheses. It is important to note that in most of the cases, acylhydrazones were obtained as (*E*)-isomers.

The gold(I) complexes **2a** and **2b** are almost equally active in hydrohydrazidation reactions. The thermal stability of gold(I)-NHC precatalysts (**2a** and **2b**) was examined using thermo-gravimetric analysis (TGA). TGA data suggested the gold(I)-NHC catalysts are stable in the catalysis temperature at 95 °C (Supporting Information Figure S11).

The synthesis of acylhydrazone derivatives by the $Ph_3PAuNTf_2$ catalyst was recently reported by Kukushkin et al. with catalyst loading of 6 mol%.[8] The reactions were performed at 60 °C, but due to its instability, the catalyst was inactive at higher temperatures as well as during longer reaction time periods. The catalysts **2a** and **2b** are highly active and have broader substrate scope at 2 mol% of catalyst loading in 6-h reaction time compared to $Ph_3PAuNTf_2$. Further, a mercury poisoning experiment was performed to investigate the homogeneous nature of the gold(I) catalyst.[11] The metallic mercury did not suppress the catalytic activity, which indicates homogeneous catalysis.

To study the cooperativity effect of bimetallic gold(I)-NHC complexes **2a** and **2b**, we used the monometallic gold(I)-NHC complexes, that is (SIPr)AuCl (SIPr = 1,3-bis(2,6-di-iso-propylphenyl)-4,5-dihydroimidazol-2-ylidene) and (IMe)AuCl (IMe =1,3-dimethylimidazol-2-ylidene) as catalysts for hydrohydrazidation reactions under the same reaction conditions (entries 9–12). We observed that the reaction yield obtained from the 2 mol% of bimetallic catalyst loading of **2a** matched up with the double catalyst loading (4 mol%) of monometallic complex (SIPr)AuCl. This observation concludes that the monometallic and bimetallic gold(I) complexes are equally active, which ruled out the possibility of cooperativity effect of bimetallic catalysts **2a** and **2b**. The two sites of bimetallic gold(I) complexes performed independently as two separate catalytic cycles in hydrohydrazidation reactions.

2.3 | Mechanistic study

The reaction mechanism of gold(I)-catalyzed nucleophilic addition to alkynes has been studied extensively by several groups.[2e,12] The detailed reaction mechanism of gold(I)-catalyzed reaction of hydrazides with alkynes was not reported so far. To gain insight into the hydrohydrazidation of terminal alkynes by gold(I)-NHC catalyst, calculations based on density functional theory (DFT) were performed to evaluate the catalyst mode of action during the process. We have already shown experimentally that the two sites of bimetallic gold(I) complexes **2a** and **2b** performed independently as two separate catalytic cycles. Therefore, we used the gold(I)-NHC complex, [1,3-dimethylimidazol-2-ylidene]AuCl, as a precatalyst, phenylacetylene, and benzohydrazide following the original reaction. Based on the earlier reports,[2e,j,3a,12g,13] we proposed a mechanism of hydrohydrazidation of terminal alkynes, which involves the formation of gold(I)-activated alkyne complex (**A**) from the reaction of NHCAuCl, $AgSbF_6$, and phenylacetylene (Scheme 2). Complex **A** further reacts with benzohydrazide (**A′**) to form the intermediate **B**, which undergoes a nucleophilic attack of hydrazide nitrogen atom at the alkyne carbon, resulting in **C**. The intermediate **C** further undergoes a proton transfer process to form a gold(I)-bound alkene species **D**. The species **D** yields the enamine **E** along with the active species **A**. Finally, the tautomerization of **E** results in the desired product **F** (Scheme 2).

Initially, a systematic conformational search was performed for all the reactants, reaction intermediates, transition states, and products using DFT-based hybrid B3LYP functional[14] with 6-31G(d) basis sets except for Au for which LanL2DZ basis with pseudo potential was used.[15] The lowest energy minima obtained from conformational search and transition states for each structure were further optimized at higher 6-31G(d,p) basis sets (for Au LanL2DZ with pseudo potential was used) with tight convergence criteria and "ultrafine" numerical grids followed by harmonic frequency calculations to

SCHEME 2 Proposed mechanism for the hydrohydrazidation of terminal alkynes

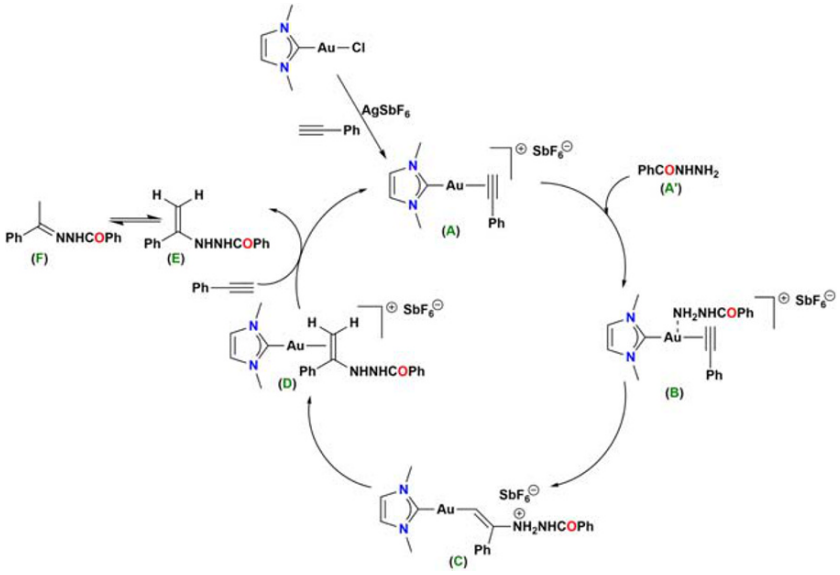

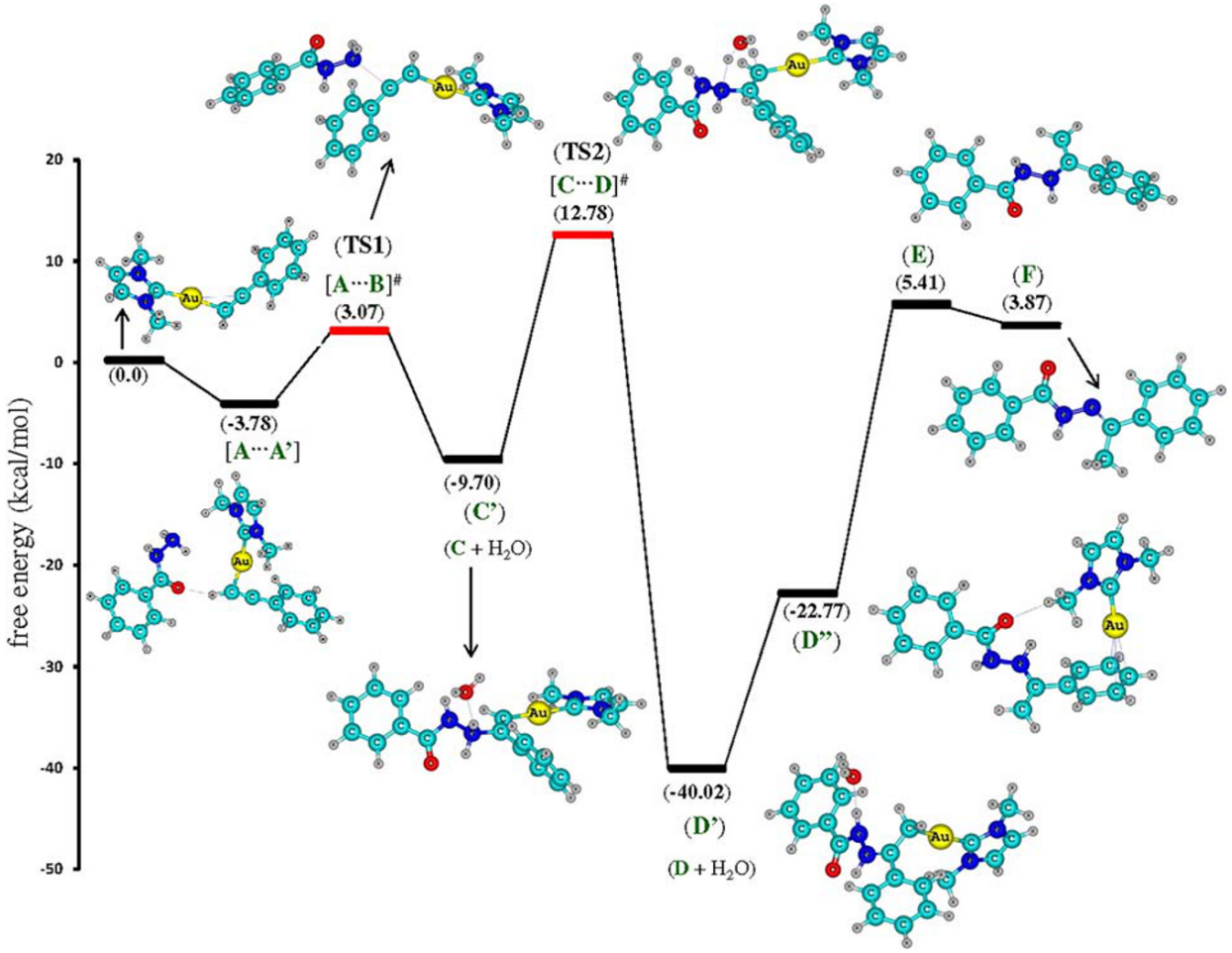

FIGURE 3 Density functional theory computed energy (kcal mol^{-1}) profile for hydrohydrazidation of phenylacetylene by a gold(I)-N heterocyclic carbene catalyst

assign each structure as a true minimum or maximum. The transition state was determined with an imaginary vibrational frequency corresponding to the reaction coordinate. To calculate the energy profile, vibrational zero-point energy was considered for all the cases. All the theoretical calculations were performed using the Gaussian16 package.[16] All the coordinates are given in Supporting Information Table S4-S15.

As shown in Scheme 2, our proposed mechanism starts with the reaction of cationic gold(I)-NHC-phenylacetylene complex (**A**) with benzohydrazide (**A′**) to form the alkyne-benzohydrazide-bound cationic intermediate species **B**. Due to the interaction of **A** with benzohydrazide, the reactive intermediate is stabilized by 3.7 kcal mol^{-1} (Figure 3). Next, the hydrazide and alkyne-bound cationic intermediate species **B** undergo a nucleophilic attack of the coordinated hydrazide nitrogen at the alkyne carbon, resulting in the C−N bond formation. During the course of reaction, subsequent changes in the Au–C bond distances with two different carbons of alkynes are observed. It has been found that the attacking carbon loses its interactions with the Au by increasing the bond length from 2.62, 2.86, and 3.08 Å, respectively, with a subsequent decrease in the C–Au bond length of the other carbon as 2.18, 2.11, and 2.04 Å, respectively, from the reactant *via* the transition state (TS) to product. The energy barrier for this step displays a low activation barrier of 6.85 kcal mol^{-1}, and the TS is characterized by an imaginary frequency of *i*53 cm^{-1} along the displacement vector in the direction of C−N bond formation. Such a low energy barrier indicates that this step occurs rapidly. The overall reaction is exothermic in nature and therefore thermodynamically favorable by ∼5.92 kcal mol^{-1}. In the next step, this species undergoes a proton transfer process between hydrazide and alkyne carbon to yield **D** *via* a four-membered TS. Before the TS, a rotation between N–N bond takes place to attain the favorable conformation where both the structures, before and after rotation, are found to have similar energies. The activation energy barrier for the proton transfer from its nearest reactant species is ∼43.1 kcal mol^{-1}, which should be high and motivated us to find an alternative lower energy path for this step. That indicates the possibility of the presence of any other adventitious molecule such as a solvent (i.e., H_2O), the prospects of which can reduce the energy barrier. We found that a water-mediated proton relay process drops down the activation barrier by half (∼22.48 kcal mol^{-1}) where the TS is a six-membered ring for the proton shuttle step (Supporting Information, Figure S40). This energy barrier is followed by a large gain in the stabilization of the species **D′**, where the overall reaction is highly exothermic by ∼30.32 kcal mol^{-1}. Note that the net energy lost due to this TS from the reaction intermediate **B** is only ∼16.56 kcal mol^{-1}. This, along with the high exothermic nature of this step, supports the formation of **D′** in the given experimental conditions. The characteristic imaginary frequency of *i*525 cm^{-1} represents an excellent displacement vector in the direction of hydrogen atom transfer from hydrazide nitrogen to alkyne carbon via a water molecule. If this alternate low-energy pathway had not been explored, the high energy barrier without the water molecule would have made the proton transfer step not viable considering the reaction conditions. As the reaction barrier for a four-membered ring is prohibitively high without water and following the actual experimental conditions, the investigation of the reaction path with an explicit water molecule is therefore rationalized. The use of explicit solvent reduced the barrier height significantly due to the formation of a six-membered ring in place of the four-membered ring, that reduced the ring strain and assisted the smooth hydrogen shuttle motion following a six-membered ring and were known in the literature.[14a,17] This observation is thus emphasized the importance of explicit solvation in understanding the mechanism of such reactions. In the next step of the catalytic cycle, gold(I)-NHC catalyst disassociates gradually from **D″** by breaking a strong bond with bond length 2.19 Å between Au and terminal alkene, thus forming a weak bond with the phenyl ring (bond length 2.40 Å) with an energy loss of 17.25 kcal mol^{-1}. This weak bond further breaks to form **E** along with a free gold(I)-NHC precatalyst, which has higher energy (28.18 kcal mol^{-1}) overall. Due to the cleavage of strong Au–C bond in this step, the energy loss becomes apparent, which is immediately compensated by the formation of another NHC-gold(I)-phenylacetylene complex **A** as the starting point of the catalytic reaction cycle. The final step of the catalytic cycle involves the tautomerization of **E** to form the final product **F,** with an energy gain of 1.54 kcal mol^{-1} (Figure 3).

3 | CONCLUSIONS

In summary, we synthesized the dinuclear gold(I)-N-heterocyclic carbene complexes and studied their catalytic activity in hydrohydrazidation of terminal alkynes. The two gold(I)-NHC complexes were fully characterized using NMR, IR, HRMS, and elemental analysis studies. One of the complexes was structurally characterized using X-ray crystallography. The gold(I)-NHC complexes efficiently (in terms of catalyst loading and regioselectivity) catalyze the hydrohydrazidation of

terminal alkynes. Also, this catalytic process can be even used for gram-scale synthesis. DFT calculations explored the details of the reaction mechanism and corresponding structural features such as the interactions of gold with other atoms and the nature of bond-breaking and bond-making processes during the course of the reaction. The energy data reveal that the barrier for the nucleophilic attack on the hydrazide and alkyne-bound cationic intermediate was very low, and the proton transfer process between hydrazide and alkyne carbon was found highly adventitious with proton relay process using an explicit solvent like water. Both the steps were found thermodynamically stable, and the hydrogen transfer process was, in particular, highly exothermic in nature. This work will further illustrate the application of gold(I)-NHC catalysts in organic synthesis, in particular for the synthesis of acylhydrazone derivatives.

4 | EXPERIMENTAL

4.1 | General procedures

All reactions were carried out under an atmosphere of nitrogen or in air. Solvents were purchased from commercial sources. NMR spectra were recorded at 298 K on a Bruker 500 MHz and JEOL 400 MHz NMR spectrometer. The chemical shifts of proton and carbon are reported in ppm and referenced using residual proton (7.26 ppm) and carbon signals (77.16 ppm) of $CDCl_3$ and residual proton (2.50 ppm) and carbon signals (39.5 ppm) of DMSO-d_6.[18] NMR annotations used: br. = broad, d = doublet, m = multiplet, s = singlet, t = triplet, sept = septet. Infrared spectra were recorded on a Perkin Elmer, Spectrum 2 spectrometer operating at 2 cm^{-1} spectral resolution. IR spectroscopic data were collected using KBr pellets. Elemental analyses were performed using a Thermo Quest FLASH 2000 SERIES (CHNS) elemental analyzer. Mass data were collected using the Micromass Q-TOF spectrometer. All catalytic reactions were monitored on a Thermo Fisher Trace 1300 series GC system by Gas Chromatography with Flame Ionization Detector (GC-FID) with a TG-IMS column of 30 m length, 0.25 mm diameter, and 0.25 μm film thickness. X-ray diffraction data for compounds **2a** were collected on a dual core Agilent Technologies (Oxford Diffraction) Super Nova CCD system. Data were collected at 293 K using graphite-monochromated CuKα radiation (λ = 1.54184 Å). The data collection strategy was interpreted by employing the CrysAlisPro software. The structure was solved using intrinsic phasing (SHELXT) and was refined by full-matrix least-squares procedures against F^2 utilizing SHELXTL (Version 6.10) software.[19] Olex2 was also used for labeling and refining of crystal **2a**. CCDC-1961139 (**2a**) contains the supplementary crystallographic data for this paper. The data can be obtained freely at www.ccdc.cam.ac.uk/conts/retrieving.html.

4.2 | Materials

NHC ligand precursors,[20] $(Ph_3P)AuCl$,[21] (SIPr)AuCl,[22] (IMe)AuCl,[23] and Au $(SMe_2)Cl$[24] were synthesized using literature procedures. $AgSbF_6$, phenylacetylene, 4-ethynyltoluene, 4-ethylphenylacetylene, 4-*tert*-butylphenylacetylene, 4-ethynylanisole, propargyl alcohol, diphenylacetyelene, benzohydrazide, 4-nitrobenzohydrazide, and 4-methoxybenzohydrazide were purchased from commercial suppliers and used as received.

-

4.3 | Syntheses

4.3.1 | Synthesis of [(*bis*-NHC^{Mes})Au_2Cl_2] complex (2a)

A mixture of imidazolium salt **1a** (0.350 g, 0.578 mmol) and Ag_2O (0.161 g, 0.694 mmol) in dichloromethane (30 mL) was stirred at room temperature for overnight. The reaction mixture was filtered through Celite, and Au $(SMe_2)Cl$ (0.341 g, 1.16 mmol) was added to it under stirring. The reaction mixture was further stirred for 10 h and filtered through Celite pad and washed with dichloromethane (2 × 5 ml). The solvent was concentrated, and hexane was added. A white precipitate obtained was washed with hexane. The residue was dried under vacuum to obtain a white solid as product **2a** (0.492 g, 85% yield). ^1H NMR (500 MHz, $CDCl_3$): δ 7.34 (s, 2H), 7.28–7.23 (m, 5H), 6.96 (s, 4H), 6.85 (s, 2H), 4.04 (t, 4H, J_{HH} = 6.7 Hz, CH_2), 3.88 (s, 2H, CH_2Ph), 3.13 (t, 4H, J_{HH} = 6.7 Hz, CH_2), 2.33 (s, 6H, *p*-$CH_3C_6H_2$), 2.02 (s, 12H, *o*-$CH_3C_6H_2$). $^{13}C\{^1H\}$ NMR (125 MHz, $CDCl_3$): δ 171.4 (Au–$C_{carbene}$), 139.6, 138.1, 134.7, 129.4, 129.0, 128.5, 127.5, 122.2, 121.4, 59.6, 54.4, 49.3, 21.1, 17.9 ppm. IR (KBr, pellet): υ_{max} 3,121(m), 3,026(w), 2,920(s), 2,852(m), 1,607(w), 1,561(w), 1,488(s), 1,451(s), 1,418(s), 1,378(w), 1,240(m), 1,143(w), 1,029(w), 854(w), 738(s), 696(m), 584(w) cm^{-1}. HRMS (ESI) calcd. For $C_{35}H_{41}Au_2ClN_5^+$ $[M\text{-}Cl]^+$ *m/z* 960.2381; found 960.2376. Anal. Calcd for $C_{35}H_{41}Au_2Cl_2N_5 \cdot 0.5CH_2Cl_2$: C, 41.04; H, 4.07; N, 6.74; found: C, 41.16; H, 4.36; N, 5.59.

4.3.2 | Synthesis of [(*bis*-NHC^{Dipp})Au_2Cl_2] complex (2b)

A mixture of imidazolium salt **1b** (0.100 g, 0.145 mmol) and Ag_2O (0.041 g, 0.176 mmol) in dichloromethane (30 mL) was stirred at room temperature for overnight. The reaction mixture was filtered through Celite, and Au(SMe_2)Cl (0.085 g, 0.290 mmol) was added to it. The reaction mixture was further stirred for 10 h and filtered through Celite pad and washed with dichloromethane (~2 × 5 mL). The solvent was concentrated to 3 ml, and hexane was added to yield a white precipitate. The white solid was further washed with hexane (~30 ml) and dried under vacuum. The product **2b** was obtained as a white solid (0.123 g, 79% yield). ^{1}H NMR (500 MHz, $CDCl_3$): δ 7.48–7.47 (m, 2H), 7.35 (s, 2H), 7.27–7.21 (m, 9H), 6.88 (s, 2H), 4.42 (t, 4H, J_{HH} = 6.7 Hz, CH_2), 3.89 (s, 2H, CH_2Ph), 3.13 (t, 4H, J_{HH} = 6.7 Hz, CH_2), 2.40 (sept, 4H, J_{HH} = 7.0 Hz, CH (CH_3)$_2$), 1.29 (d, 12H, J_{HH} = 7.0 Hz, CH (CH_3)$_2$), 1.13 (d, 12H, J_{HH} = 7.0 Hz, CH (CH_3)$_2$). ^{13}C{^{1}H} NMR (125 MHz, $CDCl_3$): δ 172.6 (Au–$C_{carbene}$), 145.7, 138.1, 134.0, 130.6, 129.0, 128.4, 127.4, 124.2, 123.4, 121.1, 59.6, 54.3, 49.1, 28.4, 24.4, 24.3 ppm. IR (KBr, pellet): υ_{max} 3,123(w), 2,961(s), 2,867(m), 1723(m), 1,663(m), 1,460(s), 1,361(w), 1,062(m), 804(w), 753(m), 698(w), 471(w) cm^{-1}. HRMS (ESI) calcd. For $C_{41}H_{53}Au_2ClN_5^+$ [M-Cl]$^+$ *m/z* 1044.3315; found 1044.3305. Anal. Calcd. for $C_{41}H_{53}Au_2Cl_2N_5$•0.3CH_2Cl_2: C, 44.76; H, 4.88; N, 6.31; found: C, 44.38; H, 4.35; N, 6.73.

4.4 | General procedure for hydrohydrazidation of alkynes

Gold(I) complex (**2a** or **2b**, 2 mol%) and $AgSbF_6$ (4 mol%) were added to a solution of benzohydrazide (1.00 mmol) and alkynes (1.20 mmol) in 2 ml of chlorobenzene in air. The reaction mixture was heated at 95 °C for 6 h. After cooling the reaction mixture at room temperature, chlorobenzene was removed under vacuum distillation, and the crude mixture was purified by column chromatography (Eluent EtOAc: petroleum ether = 40:60) to obtain the keto-*N*-acylhydrazones (**3aa**-**3an**).

4.4.1 | (*E*)-*N*′-(1-Phenylethylidene) benzohydrazide (3aa)[8]

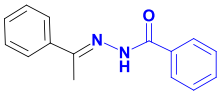

Colorless solid, m.p. = 168–169.1 °C. ^{1}H NMR (500 MHz, DMSO-d_6): δ 10.76 (s, 1H, NH), 7.88 (br. s, 4H), 7.57–7.56 (m, 1H), 7.52–7.49 (m, 2H), 7.42 (s, 3H), 2.36 (s, 3H, CH_3). ^{13}C{^{1}H} NMR (125 MHz, DMSO-d_6): δ 164.0, 155.6, 138.1, 134.1, 131.5, 129.4, 128.3, 127.9, 126.4, 14.5 ppm.

4.4.2 | (*E*)-*N*′-(1-(*p*-Tolyl)ethylidene) benzohydrazide (3ab)[8]

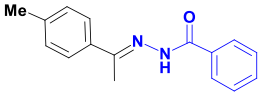

Colorless solid, m.p. = 168.3–169.0 °C. ^{1}H NMR (500 MHz, DMSO-d_6): δ 10.73 (s, 1H, NH), 7.87 (s, 2H), 7.75 (s, 2H), 7.57–7.50 (m, 3H), 7.23 (s, 2H), 2.33 (s, 6H). ^{13}C{^{1}H} NMR (125 MHz, DMSO-d_6): δ 163.9, 155.8, 139.2, 135.3, 134.1, 129.0, 128.6, 128.3, 127.8, 126.4, 20.9, 14.5 ppm.

4.4.3 | (*E*)-*N*′-(1-(4-Ethylphenyl) ethylidene)benzohydrazide (3ac)

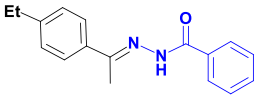

Colorless solid, m.p. = 163.0–164.6 °C. ^{1}H NMR (500 MHz, DMSO-d_6): δ 10.73 (s, 1H, NH), 7.87–7.77 (m, 4H), 7.57–7.50 (m, 3H), 7.27 (s, 2H), 2.63–2.62 (m, 2H), 2.33 (s, 3H), 1.21–1.17 (m, 3H) ppm. ^{13}C{^{1}H} NMR (100 MHz, DMSO-d_6): δ 164.7, 156.9, 146.1, 135.8, 134.1, 132.1, 128.9, 128.2, 127.9, 127.0, 28.4, 15.8, 15.0 ppm. HRMS (ESI), *m/z*: [M + H]$^+$ calcd. For $C_{17}H_{19}N_2O^+$: 267.1497; found 267.1495.

4.4.4 | (*E*)-*N*′-(1-(4-Methoxyphenyl) ethylidene)benzohydrazide (3ad)[8]

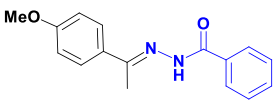

Colorless solid, m.p. = 167.8–169.0 °C. ^{1}H NMR (500 MHz, DMSO-d_6): δ 10.6 (s, 1H, NH), 7.87–7.81 (m, 4H), 7.57–7.50 (m, 3H), 6.99–6.97 (m, 2H), 3.79 (s, 3H), 2.32 (s, 3H) ppm. ^{13}C{^{1}H} NMR (100 MHz, DMSO-d_6): δ 163.8, 160.5, 156.0, 134.2, 132.6, 132.0, 131.5, 130.5, 128.4, 128.1, 127.8, 113.8, 55.3, 14.5 ppm.

4.4.5 | (*E/Z*)-4-Methoxy-*N*′-(1-phenylethylidene)benzohydrazide (3ae)[8,25]

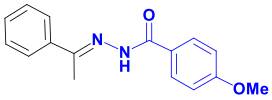

Colorless solid, m.p. = 169.0–170.9 °C. ^{1}H NMR (500 MHz, DMSO-d_6): described as a mixture of (*E/Z*) isomers, a molar ratio ~4:1, signals of minor isomer marked with asterisk, δ 10.6 (s, 1H), 10.2* (s, 0.24 H), 7.90–7.87 (m, 2H), 7.82 (br.s, 2H), 7.41 (s, 3H), 7.04–7.03 (m, 2H), 3.82 (s, 3H), 2.35 (s, 3H) ppm. ^{13}C{^{1}H} NMR (125 MHz, DMSO-d_6): δ 165.5*, 162.0, 138.2, 130.0, 129.4, 128.8, 128.4, 128.2, 126.4, 126.1, 113.8, 113.6, 55.5, 14.5 ppm.

4.4.6 | (*E*)-4-Methoxy-*N*′-(1-(*p*-tolyl) ethylidene)benzohydrazide (3af)[26]

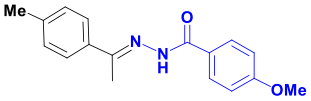

Colorless solid, m.p. = 171.6–172.2 °C. ^{1}H NMR (500 MHz, DMSO-d_6): δ 10.57 (s, 1H, NH), 7.88 (d, 2H, J_{HH} = 8.5 Hz), 7.73 (br. s, 2H), 7.23–7.22 (m, 2H), 7.04–7.02 (m, 2H), 3.82 (s, 3H), 2.32 (s, 6H). ^{13}C{^{1}H} NMR (125 MHz, DMSO-d_6): δ 161.8, 147.1, 139.0, 135.4, 131.3, 129.3, 128.9, 126.3, 126.1, 113.5, 55.4, 20.8, 14.3 ppm. Anal. Calcd for $C_{17}H_{18}N_2O_2$: C, 72.32; H, 6.43; N, 9.92; found: C, 71.97; H, 6.52; N, 8.27. HRMS (ESI), *m/z*: $[M + H]^+$ calcd. For $C_{17}H_{19}N_2O_2^+$: 283.1447; found 283.1446.

4.4.7 | (*E*)-*N*′-(1-(4-Ethylphenyl) ethylidene)-4-methoxybenzohydrazide (3ag)

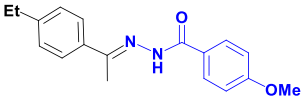

Colorless solid, m.p. = 169.4–170.1 °C. ^{1}H NMR (500 MHz, DMSO-d_6): δ 10.5 (s, 1H, NH), 7.88 (d, 2H, J_{HH} = 8.5 Hz), 7.75 (br. s, 2H), 7.26–7.24 (m, 2H), 7.03 (d, 2H, J_{HH} = 8.5 Hz), 3.82 (s, 3H), 2.62 (q, 2H, J_{HH} = 7.5 Hz), 2.33 (s, 3H), 1.18 (t, 3H, J_{HH} = 7.5 Hz) ppm. ^{13}C{^{1}H} NMR (125 MHz, DMSO-d_6): δ 161.8, 145.2, 135.7, 131.3, 129.8, 127.7, 126.4, 126.1, 113.8, 113.5, 55.4, 27.9, 15.4, 14.4 ppm. Anal. Calcd for $C_{18}H_{20}N_2O_2$: C, 72.95; H, 6.80; N, 9.45; found: C, 72.76; H, 6.14; N, 9.82. HRMS (ESI), *m/z*: $[M + H]^+$ calcd. For $C_{18}H_{21}N_2O_2^+$: 297.1603; found 297.1603.

4.4.8 | (*E*)-*N*′-(1-(4-(*t*-butyl)phenyl) ethylidene)-4-methoxybenzohydrazide (3ah)

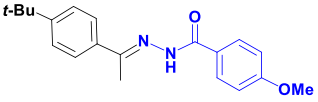

Colorless solid, m.p. = 182.3–183.1 °C. ^{1}H NMR (500 MHz, DMSO-d_6):10.5 (s, 1H), 7.87 (d, 2H, J_{HH} = 8.5 Hz), 7.74 (br. s, 2H), 7.43 (d, 2H, J_{HH} = 8.5 Hz), 7.03 (d, 2H, J_{HH} = 8.5 Hz), 3.82 (s, 3H), 2.32 (s, 3H), 1.28(s, 3H) ppm. ^{13}C{^{1}H} NMR (125 MHz, DMSO-d_6): δ 161.9, 152.1, 135.5, 129.8, 126.2, 125.2, 113.9, 113.6, 55.5, 34.5, 31.09, 14.4 ppm. HRMS (ESI), *m/z*: $[M + H]^+$ calcd. For $C_{20}H_{25}N_2O_2^+$: 325.1916; found 325.1915.

4.4.9 | (*E/Z*)-4-Methoxy-*N*′-(1-(4-methoxyphenyl)ethylidene) benzohydrazide (3ai)[26]

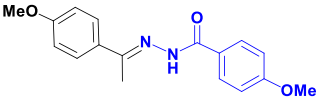

Colorless solid, m.p. = 172.3–173.1 °C. ^{1}H NMR (500 MHz, DMSO-d_6): described as a mixture of (*E/Z*) isomers, a molar ratio ~3.7:1, signals of minor isomer marked with asterisk, δ 10.5 (s, 1H), 10.2* (s, 0.27 H), 7.91–7.86 (m, 2H), 7.79 (br.s, 2H), 7.04–7.02 (m, 2H), 6.98–6.96 (m, 2H), 3.82 (s, 3H), 3.79* (s, 2.3H), 2.31 (s, 3H) ppm. ^{13}C{^{1}H} NMR (100 MHz, DMSO-d_6): δ 165.5, 162.0, 161.8, 160.4, 130.6, 129.7, 129.4, 127.9, 126.2, 124.8, 113.7, 55.4, 55.3, 14.4 ppm. HRMS (ESI), *m/z*: $[M + H]^+$ calcd. For $C_{17}H_{19}N_2O_3^+$: 299.1396; found 299.1399.

4.4.10 | (*E*)-4-Nitro-*N*′-(1-phenylethylidene)benzohydrazide (3aj)[8]

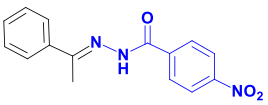

Pale-yellow solid, m.p. = 197.6–198.0 °C. ^{1}H NMR (500 MHz, DMSO-d_6): δ 11.0 (s, 1H), 8.35–8.33 (m, 2H),

8.13–8.12 (m, 2H), 7.87 (s, 2H), 7.44 (s, 3H), 2.39 (s, 3H) ppm. $^{13}C\{^1H\}$ NMR (125 MHz, DMSO-d_6): δ 162.5, 156.9, 149.1, 139.8, 137.8, 129.7, 129.4, 128.4, 126.5, 123.4, 14.8 ppm. HRMS (ESI), *m/z*: $[M + H]^+$ calcd. For $C_{15}H_{14}N_3O_3^+$: 284.1035; found 284.1034.

4.4.11 | (*E*)-4-Nitro-*N*′-(1-(*p*-tolyl) ethylidene)benzohydrazide (3ak)[27]

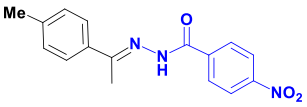

Pale-yellow solid, m.p. = 214.2–215.6 °C. ^1H NMR (500 MHz, DMSO-d_6):11.05 (s, 1H), 8.34–8.33 (m, 2H), 8.12–8.10 (m, 2H), 7.77–7.76 (m, 2H), 7.25–7.24 (m, 2H), 2.35–2.34 (m, 6H) ppm. $^{13}C\{^1H\}$ NMR (125 MHz, DMSO-d_6): δ 162.4, 157.1, 149.1, 139.9, 139.5, 135.1, 129.4, 129.0, 126.5, 123.4, 20.8, 14.8 ppm. HRMS (ESI), *m/z*: $[M + H]^+$ calcd. For $C_{16}H_{16}N_3O_3^+$: 298.1192; found 298.1190.

4.4.12 | (*E*/*Z*)-N′-(1-(4-Ethylphenyl) ethylidene)-4-nitrobenzohydrazide (3al)

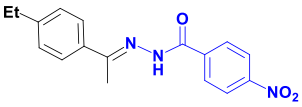

Pale-yellow solid, m.p. = 220.3–221.8 °C. ^1H NMR (500 MHz, DMSO-d_6): described as a mixture of (*E*/*Z*) isomers, a molar ratio ∼2.9:1, signals of minor isomer marked with asterisk, δ 11.04 (s, 1H), 11.0* (s, 0.34H), 8.38–8.37 (m, 1H), 8.34–8.32 (m, 2H), 8.16–8.15 (m, 1H), 8.12–8.11 (m, 2H), 7.79–7.78 (m, 2H), 7.28–7.27 (m, 2H), 2.64–2.63 (m, 3H), 2.36 (s, 3H), 1.21–1.18 (m, 5H) ppm. $^{13}C\{^1H\}$ NMR (100 MHz, DMSO-d_6): δ162.4, 157.1, 149.1, 145.8, 135.3, 129.4, 129.1, 127.8, 126.7, 123.9, 123.5, 28.0, 15.4, 14.8 ppm. HRMS (ESI), *m/z*: $[M + H]^+$ calcd. For $C_{17}H_{18}N_3O_3^+$: 312.1348; found 312.1345.

4.4.13 | (*E*)-*N*′-(1-(4-Methoxyphenyl) ethylidene)-4-nitrobenzohydrazide (3am)[27]

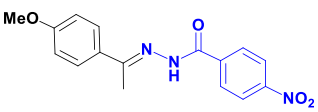

Pale-yellow solid, m.p. = 216.6–217.0 °C. ^1H NMR (500 MHz, DMSO-d_6):11.00 (s, 1H), 8.39–8.33 (m, 2H), 8.16–8.10 (m, 2H), 7.84–7.83 (m, 2H), 7.01–6.99 (m, 2H), 3.80 (s, 3H), 2.34 (s, 3H) ppm. $^{13}C\{^1H\}$ NMR (100 MHz, DMSO-d_6): δ 164.3, 160.7, 157.2, 149.5, 129.4, 129.1, 128.2, 123.9, 123.5, 113.8, 55.3, 14.7 ppm. HRMS (ESI), *m/z*: $[M + H]^+$ calcd. For $C_{16}H_{16}N_3O_4^+$: 314.1141; found 314.1144.

4.4.14 | (*E*)-*N*′-(1-Hydroxypropan-2-ylidene)benzohydrazide (3an)

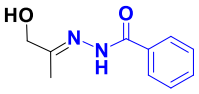

Colorless solid, m.p. = 126.0–128.3 °C. ^1H NMR (500 MHz, DMSO-d_6): δ 10.51 (s, 1H, NH), 7.92 (s, 1H), 7.92–7.91 (m, 2H), 7.61–7.58 (m, 1H), 7.54–7.51 (m, 2H), 1.29 (s, 2H), 1.25 (s, 3H) ppm. $^{13}C\{^1H\}$ NMR (125 MHz, $CDCl_3$): δ 166.3, 133.0, 132.3, 129.0, 127.9, 31.6, 22.5 ppm.

4.5 | Mercury poisoning experiment

Gold(I) complex (**2a**, 2 mol%) and $AgSbF_6$ (4 mol%) were added to a solution of benzohydrazide (1.00 mmol) and phenylacetylene (1.20 mmol) in 2 ml of chlorobenzene. Excess Hg(0) (500 times with respect to catalyst loading) was added. The reaction mixture was heated at 95 °C for 6 h and was cooled to room temperature. DMSO (2 ml) was added to make a clear solution. The product was analyzed using GC, and yield was determined based on 1,3,5-trimethoxybenzene as an internal standard. The result showed no significant decrease in the product yield under the same conditions.

4.6 | Gram-scale synthesis of (*E*)-*N*′-(1-phenylethylidene)benzohydrazide (3aa)

Gold(I) complex (**2a**, 2 mol%) and $AgSbF_6$ (4 mol%) were added to a solution of benzohydrazide (1.00 g, 7.34 mmol) and phenylacetylene (0.899 g, 8.81 mmol) in 15 ml of chlorobenzene. The reaction mixture was heated at 95 °C for 6 h and was cooled to room temperature. The solvent was removed under vacuum distillation, and the crude mixture was purified using column chromatography using ethyl acetate/petroleum ether solvent system to obtain the desired product **3aa** as a colorless solid (1.57 g, 90% yield).

ACKNOWLEDGEMENTS

This work was supported by the DST-SERB, New Delhi (Grant Number: YSS/2014/000054). S.Y. thanks Central University of Rajasthan for the research fellowship. The

authors thank DST-FIST (Grant Number: SR/FST/CSI-257/2014(c)) for providing instrumental facilities. The authors acknowledge the IIT Bombay and Materials Research Centre, MNIT, Jaipur for collecting IR and HRMS data.

CONFLICTS OF INTEREST

The authors declare no competing financial interest.

ORCID

Shaikh M. Mobin https://orcid.org/0000-0002-2665-5123
Chandrakanta Dash https://orcid.org/0000-0002-6945-1366

REFERENCES

[1] a) C. Praveen, *Coord. Chem. Rev.* **2019**, *392*, 1; b) C. Praveen, *Catal. Rev.* **2019**, *61*, 406; c) A. Fürstner, *Angew. Chem. Int. Ed.* **2018**, *57*, 4215; d) Z. Zheng, Z. Wang, Y. Wang, L. Zhang, *Chem. Soc. Rev.* **2016**, *45*, 4448; e) W. Li, B. Yu, *Chem. Soc. Rev.* **2018**, *47*, 7954; f) A. M. Asiri, A. S. K. Hashmi, *Chem. Soc. Rev.* **2016**, *45*, 4471; g) D. Pflästerer, A. S. K. Hashmi, *Chem. Soc. Rev.* **2016**, *45*, 1331; h) R. Dorel, A. M. Echavarren, *Chem. Rev.* **2015**, *115*, 9028; i) A. S. K. Hashmi, *Acc. Chem. Res.* **2014**, *47*, 864; j) A. Corma, A. Leyva-Pérez, M. J. Sabater, *Chem. Rev.* **2011**, *111*, 1657; k) N. Marion, S. P. Nolan, *Chem. Soc. Rev.* **2008**, *37*, 1776; l) A. S. K. Hashmi, *Chem. Rev.* **2007**, *107*, 3180; m) S. P. Nolan, *Acc. Chem. Res.* **2011**, *44*, 91.

[2] a) Y. Fukuda, K. Utimoto, H. Nozaki, *Heterocycles* **1987**, *25*, 297; b) Y. Fukuda, K. Utimoto, *Synthesis* **1991**, *1991*, 975; c) D. P. Zimin, D. V. Dar'in, A. A. Eliseeva, A. S. Novikov, V. A. Rassadin, V. Y. Kukushkin, *Eur. J. Org. Chem.* **2019**, *2019*, 6094; d) O. S. Morozov, P. S. Gribanov, A. F. Asachenko, P. V. Dorovatovskii, V. N. Khrustalev, V. B. Rybakov, M. S. Nechaev, *Adv. Synth. Catal.* **2016**, *358*, 1463; e) C. Dash, M. M. Shaikh, R. J. Butcher, P. Ghosh, *Inorg. Chem.* **2010**, *49*, 4972; f) R. Manzano, T. Wurm, F. Rominger, A. S. K. Hashmi, *Chem. A Eur. J.* **2014**, *20*, 6844; g) R. Kinjo, B. Donnadieu, G. Bertrand, *Angew. Chem. Int. Ed.* **2011**, *50*, 5560; h) K. D. Hesp, M. Stradiotto, *J. Am. Chem. Soc.* **2010**, *132*, 18026; i) H. Duan, S. Sengupta, J. L. Petersen, N. G. Akhmedov, X. Shi, *J. Am. Chem. Soc.* **2009**, *131*, 12100; j) E. Mizushima, T. Hayashi, M. Tanaka, *Org. Lett.* **2003**, *5*, 3349; k) S. Kramer, K. Dooleweerdt, A. T. Lindhardt, M. Rottländer, T. Skrydstrup, *Org. Lett.* **2009**, *11*, 4208; l) H. Yang, F. P. Gabbaï, *J. Am. Chem. Soc.* **2015**, *137*, 13425.

[3] a) A. Couce-Rios, G. Kovács, G. Ujaque, A. Lledós, *ACS Catal.* **2015**, *5*, 815; b) X. Zeng, G. D. Frey, S. Kousar, G. Bertrand, *Chem. A Eur. J.* **2009**, *15*, 3056; c) E. Alvarado, A. C. Badaj, T. G. Larocque, G. G. Lavoie, *Chem. A Eur. J.* **2012**, *18*, 12112; d) L.-A. Schaper, X. Wei, S. J. Hock, A. Pöthig, K. Öfele, M. Cokoja, W. A. Herrmann, F. E. Kühn, *Organometallics* **2013**, *32*, 3376; e) D. R. Tolentino, L. Jin, M. Melaimi, G. Bertrand, *Chem. Asian J.* **2015**, *10*, 2139.

[4] a) M. Baron, E. Battistel, C. Tubaro, A. Biffis, L. Armelao, M. Rancan, C. Graiff, *Organometallics* **2018**, *37*, 4213; b) V. Vreeken, D. L. J. Broere, A. C. H. Jans, M. Lankelma, J. N. H. Reek, M. A. Siegler, J. I. van der Vlugt, *Angew. Chem. Int. Ed.* **2016**, *55*, 10042; c) M. D. Levin, F. D. Toste, *Angew. Chem. Int. Ed.* **2014**, *53*, 6211.

[5] a) S. Yadav, A. Singh, N. Rashid, M. Ghotia, T. K. Roy, P. P. Ingole, S. Ray, S. M. Mobin, C. Dash, *ChemistrySelect* **2018**, *3*, 9469; b) R. S. Chauhan, D. Oza, S. Yadav, C. Dash, A. M. Z. Slawin, N. Shivran, *New J. Chem.* **2019**, *43*, 2381.

[6] S. Yadav, A. Singh, I. Mishra, S. Ray, S. M. Mobin, C. Dash, *Appl. Organomet. Chem.* **2019**, *33*, e4936.

[7] a) N. Gupta, M. Badeaux, Y. Liu, K. Naxerova, D. Sgroi, L. L. Munn, R. K. Jain, I. Garkavtsev, *Proc. Natl. Acad. Sci.* **2017**, *114*, 1033; b) J. Xi, S. Xu, L. Wu, T. Ma, R. Liu, Y.-C. Liu, D. Deng, Y. Gu, J. Zhou, F. Lan, X. Zha, *Bioorg. Chem.* **2017**, *72*, 182; c) K. Hrušková, E. Potůčková, T. Hergeselová, L. Liptáková, P. Hašková, P. Mingas, P. Kovaříková, T. Šimůnek, K. Vávrová, *Eur. J. Med. Chem.* **2016**, *120*, 97; d) S. Barman, L. You, R. Chen, V. Codrea, G. Kago, R. Edupuganti, J. Robertus, R. M. Krug, E. V. Anslyn, *Eur. J. Med. Chem.* **2014**, *71*, 81; e) R. Kulandasamy, A. V. Adhikari, J. P. Stables, *Eur. J. Med. Chem.* **2009**, *44*, 3672.

[8] D. P. Zimin, D. V. Dar'in, V. A. Rassadin, V. Y. Kukushkin, *Org. Lett.* **2018**, *20*, 4880.

[9] a) G. C. Fortman, S. P. Nolan, *Chem. Soc. Rev.* **2011**, *40*, 5151; b) D. J. D. Wilson, S. A. Couchman, J. L. Dutton, *Inorg. Chem.* **2012**, *51*, 7657.

[10] M. K. Samantaray, C. Dash, M. M. Shaikh, K. Pang, R. J. Butcher, P. Ghosh, *Inorg. Chem.* **2011**, *50*, 1840.

[11] a) D. R. Anton, R. H. Crabtree, *Organometallics* **1983**, *2*, 855; b) J. A. Widegren, R. G. Finke, *J. Mol. Catal. A: Chem.* **2003**, *198*, 317.

[12] a) J. Moran, S. I. Gorelsky, E. Dimitrijevic, M.-E. Lebrun, A.-C. Bédard, C. Séguin, A. M. Beauchemin, *J. Am. Chem. Soc.* **2008**, *130*, 17893; b) A. M. Beauchemin, J. Moran, M.-E. Lebrun, C. Séguin, E. Dimitrijevic, L. Zhang, S. I. Gorelsky, *Angew. Chem. Int. Ed.* **2008**, *47*, 1410; c) M. Pernpointner, A. S. K. Hashmi, *J. Chem. Theory Comput.* **2009**, *5*, 2717; d) M. Lein, M. Rudolph, S. K. Hashmi, P. Schwerdtfeger, *Organometallics* **2010**, *29*, 2206; e) C. M. Krauter, A. S. K. Hashmi, M. Pernpointner, *ChemCatChem* **2010**, *2*, 1226; f) G. Kovács, A. Lledós, G. Ujaque, *Angew. Chem. Int. Ed.* **2011**, *50*, 11147; g) A. Zhdanko, M. E. Maier, *Angew. Chem. Int. Ed.* **2014**, *53*, 7760.

[13] a) M. Katari, M. N. Rao, G. Rajaraman, P. Ghosh, *Inorg. Chem.* **2012**, *51*, 5593; b) G. Ciancaleoni, S. Rampino, D. Zuccaccia, F. Tarantelli, P. Belanzoni, L. Belpassi, *J. Chem. Theory Comput.* **2014**, *10*, 1021; c) V. Lavallo, G. D. Frey, B. Donnadieu, M. Soleilhavoup, G. Bertrand, *Angew. Chem. Int. Ed.* **2008**, *47*, 5224; d) Z. Lu, G. B. Hammond, B. Xu, *Acc. Chem. Res.* **2019**, *52*, 1275.

[14] a) A. D. Becke, *J. Chem. Phys.* **1993**, *98*, 5648; b) C. Lee, W. Yang, R. G. Parr, *Phys. Rev. B* **1988**, *37*, 785.

[15] a) T. Clark, J. Chandrasekhar, G. W. Spitznagel, P. V. R. Schleyer, *J. Comput. Chem.* **1983**, *4*, 294; b) M. J. Frisch, J. A. Pople, J. S. Binkley, *J. Chem. Phys.* **1984**, *80*, 3265.

[16] M. J. Frisch, G. W. Trucks, H. B. Schlegel, G. E. Scuseria, M. A. Robb, J. R. Cheeseman, G. Scalmani, V. Barone, G. A. Petersson, H Nakatsuji, X. Li. *Gaussian 16, Revision A.03*, Wallingford, CT, **2016**.

[17] R. Joshi, A. Kumawat, S. Singh, T. K. Roy, R. T. Pardasani, *J. Heterocyclic Chem.* **2018**, *55*, 1783.

[18] G. R. Fulmer, A. J. M. Miller, N. H. Sherden, H. E. Gottlieb, A. Nudelman, B. M. Stoltz, J. E. Bercaw, K. I. Goldberg, *Organometallics* **2010**, *29*, 2176.
[19] a) O. V. Dolomanov, L. J. Bourhis, R. J. Gildea, J. A. K. Howard, H. Puschmann, *J. Appl. Cryst.* **2009**, *42*, 339; b) G. M. Sheldrick, *Acta Crystallogr.* **2015**, *A71*, 3.
[20] a) J. Houghton, G. Dyson, R. E. Douthwaite, A. C. Whitwood, B. M. Kariuki, *Dalton Trans.* **2007**, 3065; b) G. A. Filonenko, M. J. B. Aguila, E. N. Schulpen, R. van Putten, J. Wiecko, C. Müller, L. Lefort, E. J. M. Hensen, E. A. Pidko, *J. Am. Chem. Soc.* **2015**, *137*, 7620.
[21] M. I. Bruce, B. K. Nicholson, O. B. Shawkataly, J. R. Shapley, T. Henly, *Inorg. Synth.* **1989**, *26*, 324.
[22] P. de Frémont, N. M. Scott, E. D. Stevens, S. P. Nolan, *Organometallics* **2005**, *24*, 2411.
[23] C. Nieto-Oberhuber, M. P. Muñoz, S. López, E. Jiménez-Núñez, C. Nevado, E. Herrero-Gómez, M. Raducan, A. M. Echavarren, *Chem. A Eur. J.* **2006**, *12*, 1677.
[24] M.-C. Brandys, M. C. Jennings, R. J. Puddephatt, *J. Chem. Soc. Dalton Trans.* **2000**, 4601.
[25] M. J. Burk, J. E. Feaster, *J. Am. Chem. Soc.* **1992**, *114*, 6266.
[26] W. Kantlehner, P. Speh, J. H. Braeuner, E. Haug, W. W. Mergen, *Chem.-Ztg.* **1990**, *114*, 179.
[27] P. Grammaticakis, *Bull. Soc. Chim. Fr.* **1970**, 933.

SUPPORTING INFORMATION

Additional supporting information may be found online in the Supporting Information section at the end of this article.

How to cite this article: Yadav S, Ray S, Singh A, Mobin SM, Roy TK, Dash C. Dinuclear gold(I)-N-heterocyclic carbene complexes: Synthesis, characterization, and catalytic application for hydrohydrazidation of terminal alkynes. *Appl Organomet Chem*. 2020;e5942. https://doi.org/10.1002/aoc.5942